

LETTERS

Efficient Generation of the Ligand Field Excited State of Tris-(2,2'-bipyridine)-ruthenium(II) through Sequential Two-Photon Capture by $[\text{Ru}(\text{bpy})_3]^{2+}$ or Electron Capture by $[\text{Ru}(\text{bpy})_3]^{3+}$

David W. Thompson, James F. Wishart, Bruce S. Brunschwig,* and Norman Sutin*

Departments of Chemistry, Brookhaven National Laboratory, Upton, New York 11973-5000, and Rutgers University, Piscataway, New Jersey 08854-8087

Received: May 14, 2001; In Final Form: July 18, 2001

The relaxation dynamics and product distribution resulting from the decay of high lying excited states generated via sequential two-photon capture by $[\text{Ru}(\text{bpy})_3]^{2+}$ or electron capture by $[\text{Ru}(\text{bpy})_3]^{3+}$ have been investigated by flash photolysis and pulse radiolysis techniques. In comparison to the decay dynamics for monophotonic excitation, dramatically different relaxation dynamics have been observed. High-power flash excitation yields both the lowest lying metal-to-ligand charge transfer ($^3\text{MLCT}$) state *and* a new transient photoproduct associated with nonradiative decay through the photodissociative metal-centered (^3dd) excited state/s. The photoproduct is postulated to be $[\text{Ru}^{\text{II}}(\text{bpy})_2(\eta^1\text{-bpy})]^{2+}$ where the pendant pyridine has rotated to yield a transient that is stabilized by a π -bonded or a three-centered Ru-C-H agostic interaction.

Introduction

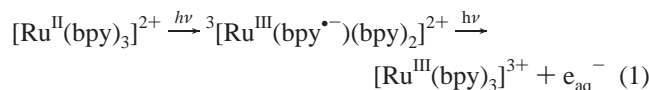
The photophysics and photochemistry of d^6 polypyridyl complexes of Re(I), Ru(II), and Os(II) have been intensely studied over the last 25 years.¹ The tris-(2,2'-bipyridine) ruthenium(II) complex has served as the paradigm for this class of compounds. Light absorption by $[\text{Ru}(\text{bpy})_3]^{2+}$ results in the formation of a Franck-Condon singlet metal-to-ligand charge-transfer ($^1\text{MLCT}$) excited state which undergoes subpicosecond intersystem crossing to a long-lived $^3\text{MLCT}$ excited state.² The $^3\text{MLCT}$ excited states, although generally substitutionally inert, can undergo facile electron and energy transfer chemistry. It is these properties that have been exploited in the construction of molecular assemblies for artificial photosynthetic purposes.³ One pathway for deactivation of the lowest lying $^3\text{MLCT}$ state is via the metal-centered ^3dd excited state.⁴ This state, although generally slightly higher in energy than the lowest lying $^3\text{MLCT}$ state, can be formed by thermal activation from the $^3\text{MLCT}$ state or via direct intersystem crossing from the $^1\text{MLCT}$ Franck-Condon state. The metal-centered ^3dd excited states are not substitutionally inert and may undergo ligand loss.⁴ The

resulting photolability limits the utility of $[\text{Ru}(\text{bpy})_3]^{2+}$ in photosynthetic applications.

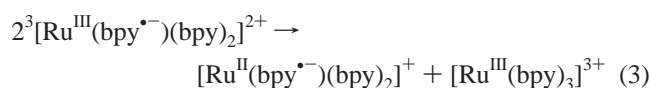
The ligand field transitions in $[\text{Ru}(\text{bpy})_3]^{2+}$ and related complexes are obscured by the much more intense charge transfer and intraligand transitions. Consequently, it is difficult to directly populate and study the ^3dd states. The participation of ^3dd excited states in the nonradiative decay of the triplet state of $[\text{Ru}(\text{bpy})_3]^{2+}$ is inferred from temperature-dependent emission yield and lifetime measurements, and the observation of photodecomposition. Prolonged irradiation or photolysis into the lowest energy MLCT band of $[\text{Ru}^{\text{II}}(\text{bpy})_3]^{2+}$ in H_2O results in spectral changes consistent with the formation of $[\text{Ru}^{\text{II}}(\text{bpy})_2(\text{H}_2\text{O})_2]^{2+}$ presumed to arise through bpy loss from the ^3dd state. To date, however, the ^3dd excited states in $[\text{Ru}(\text{bpy})_3]^{2+}$ have *not been directly observed by spectroscopic techniques*. Insight into the behavior and properties of the ^3dd excited states in $[\text{Ru}(\text{bpy})_3]^{2+}$ would be possible if the states could be generated in high yield. Two approaches, the population of the ^3dd state via two-photon excitation⁵ and the radiolytic reduction of the oxidized complex,⁶ appear promising in this regard.

* To whom correspondence should be addressed.

Two-photon excitation of Ru(II) polypyridyl complexes has received less attention than monophotonic studies. According to Meisel et al., 300–340 nm flash photolysis of aqueous solutions of $[\text{Ru}^{\text{II}}(\text{bpy})_3]^{2+}$ yields $[\text{Ru}^{\text{III}}(\text{bpy})_3]^{3+}$ and $[\text{Ru}^{\text{II}}(\text{bpy}^{\bullet-})(\text{bpy})_2]^{2+}$.^{5d,e} It was proposed that these products are formed via sequential two-photon absorption that results in the photoejection of an electron as shown in eqs 1 and 2.



The photoejection yields were small (0.0015 per ³MLCT state formed) and could be increased by the addition of sodium dodecyl sulfate.⁷ However, this interpretation has been questioned because the same products can also be formed via the disproportionation of two MLCT excited states, eq 3:⁸



Recently, Castellano and Lackowicz demonstrated that intense 90 fs, 880 nm laser excitation resulted in simultaneous two-photon absorption and the ultimate formation of the same ³MLCT excited state as produced in monophotonic 460 nm excitation.^{5b} In the related $[\text{Ru}^{\text{II}}(\text{NH}_3)_5\text{L}]^{2+}$ (L = pyridyl) family of complexes,⁹ multiphoton absorption resulted in increased photoaquation yields consistent with efficient intersystem crossing to high lying metal-centered excited states. Interestingly, photoejection of electrons in $[\text{Ru}^{\text{II}}(\text{NH}_3)_5\text{L}]^{2+}$ systems was not observed. Two-photon photochemistry has also been documented in Re(I),^{5a} Cu(I),^{5c} and Ru(II)^{5f} polypyridyl complexes as well as in dimolybdenum complexes.^{5g}

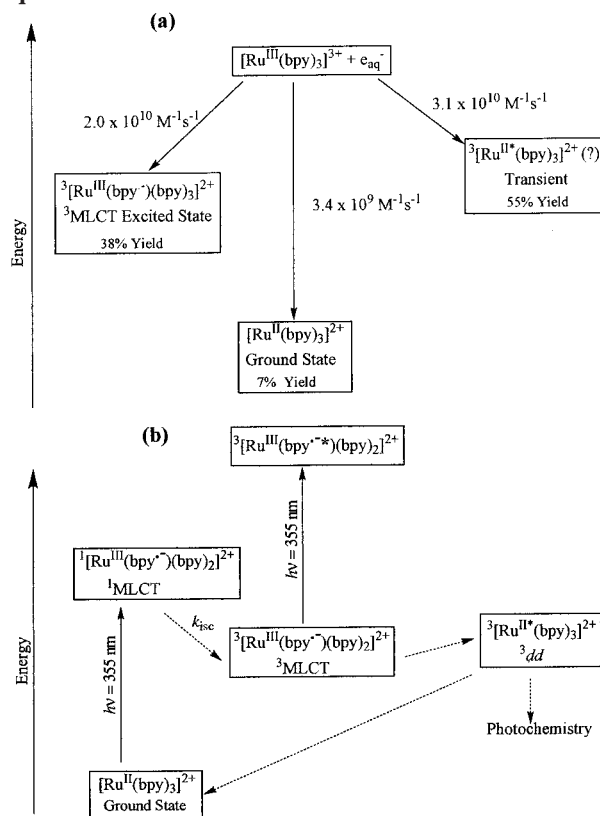
The capture of a solvated electron by $[\text{Ru}^{\text{III}}(\text{bpy})_3]^{3+}$ to form the reduced ground-state complex is very exergonic, $\Delta G^\circ = -4.1$ eV. Pulse radiolysis studies have shown that electron capture by $[\text{Ru}^{\text{III}}(\text{bpy})_3]^{3+}$ occurs at a near diffusion-controlled rate to form three species: the ground-state complex; the ³MLCT excited state, and a nonemitting species that does not exhibit significant differential absorption in the visible spectral region, Scheme 1a.⁶

The yield of the nonemitting species was 55%, based on dosimetry and kinetic modeling. Although the identity of the transient was unclear the authors speculated that it might be another excited state or a coordinated radical complex.⁶ Evidently, both pulse radiolysis and two-photon absorption afford valuable opportunities for exploring the excited-state manifold of $\text{Ru}(\text{bpy})_3^{2+}$ and related complexes. The results of experiments along these lines are described below.

Results and Discussion

Pulse Radiolysis Experiments. The electron capture experiments were performed with 2 MeV electrons from a Van de Graaff accelerator¹⁰ under the conditions used by Meisel et al.: $[t\text{-BuOH}] = 0.3$ M, $[\text{Na}_2\text{SO}_4] = 0.5$ M, and pH = 4.6 maintained with acetate buffer ($[\text{HOAc}] = 20$ mM, $[\text{NaOAc}] = 20$ mM). Pulse radiolysis of aqueous solutions generates e_{aq}^- , OH^\bullet radicals, H^\bullet atoms, H_2 , and H_2O_2 . In acidic media, the hydrated electron is converted into a H atom through reaction with a proton with $k_{\text{obsd}} = 5.5 \times 10^5$ s⁻¹ at pH 4.6. The hydroxyl radicals and H atoms formed in the pulse radiolysis rapidly react with the *t*-BuOH to form a C-centered butanol radical ($\text{C}^\bullet\text{H}_2$)(CH₃)₂C(OH) and H₂O or H₂, respectively.

SCHEME 1: (a) Electron Capture by $[\text{Ru}^{\text{III}}(\text{bpy})_3]^{3+}$. (b) Sequential Two-Photon Excitation



Electron capture by HOAc occurs with $k_{\text{obsd}} \sim 10^6$ s⁻¹ under the conditions used.

The reaction of e_{aq}^- with $[\text{Ru}^{\text{III}}(\text{bpy})_3]^{3+}$ was detected at 650 nm where e_{aq}^- has a strong absorption. The observed rates for electron capture by $[\text{Ru}^{\text{III}}(\text{bpy})_3]^{3+}$ were $\sim 7 \times 10^6$ s⁻¹. The kinetics following electron capture were multiphasic and adequately described with a biexponential function. The difference spectrum at 1 μs has a maximum at 360 nm ($\epsilon = 6000$ M⁻¹ cm⁻¹) and a broad positive absorption feature between 470 and 540 nm ($\epsilon \approx 1000$ – 2000 M⁻¹ cm⁻¹).¹¹ The absorption changes evolve with time ultimately yielding the spectrum of $[\text{Ru}^{\text{II}}(\text{bpy})_3]^{2+}$. Transient absorption studies thus indicate that an intermediate spectrally *distinct* from $[\text{Ru}^{\text{II}}(\text{bpy})_3]^{2+}$ is formed by radiolytic reduction of $[\text{Ru}^{\text{III}}(\text{bpy})_3]^{3+}$ on the microsecond time scale. These findings are consistent with the results reported by Meisel et al.⁶

Two-Photon Excitation of $[\text{Ru}^{\text{II}}(\text{bpy})_3]^{2+}$.¹² The dependence of the emission yields from the ³MLCT excited state (designated as ³ $[\text{Ru}^{\text{III}}(\text{bpy}^{\bullet-})(\text{bpy})_2]^{2+}$ below) on laser power affords a valuable mechanistic probe. Very different excitation power dependences have been demonstrated for formation of ³ $[\text{Ru}^{\text{III}}(\text{bpy}^{\bullet-})(\text{bpy})_2]^{2+}$ following monophotonic excitation at 470 nm^{13a,b} and simultaneous biphotonic excitation at 880 nm.^{5b} In the present work, the power dependence of the emission from ³ $[\text{Ru}^{\text{III}}(\text{bpy}^{\bullet-})(\text{bpy})_2]^{2+}$ (5 μM $[\text{Ru}^{\text{II}}(\text{bpy})_3]\text{Cl}_2$ in Ar saturated H₂O at 298 K unless otherwise noted) provides evidence for sequential two 355 nm photon absorption as shown in Scheme 1b.^{13,14} In this mechanism, absorption of a single photon in the MLCT band ($\epsilon_{355} = 6500$ M⁻¹ cm⁻¹) creates the ¹MLCT excited state. Intersystem crossing to form the emissive ³MLCT excited state is efficient ($\phi_{\text{isc}} = 1$) and occurs on an ultrafast time scale ($\tau < 200$ fs, $k > 5 \times 10^{12}$ s⁻¹).² The ³MLCT excited state produced is long-lived ($\tau = 530$ ns, $k = 1.9 \times 10^6$ s⁻¹) and absorbs strongly at 355 ($\epsilon_{355} = 22000$ M⁻¹ cm⁻¹) and at 460

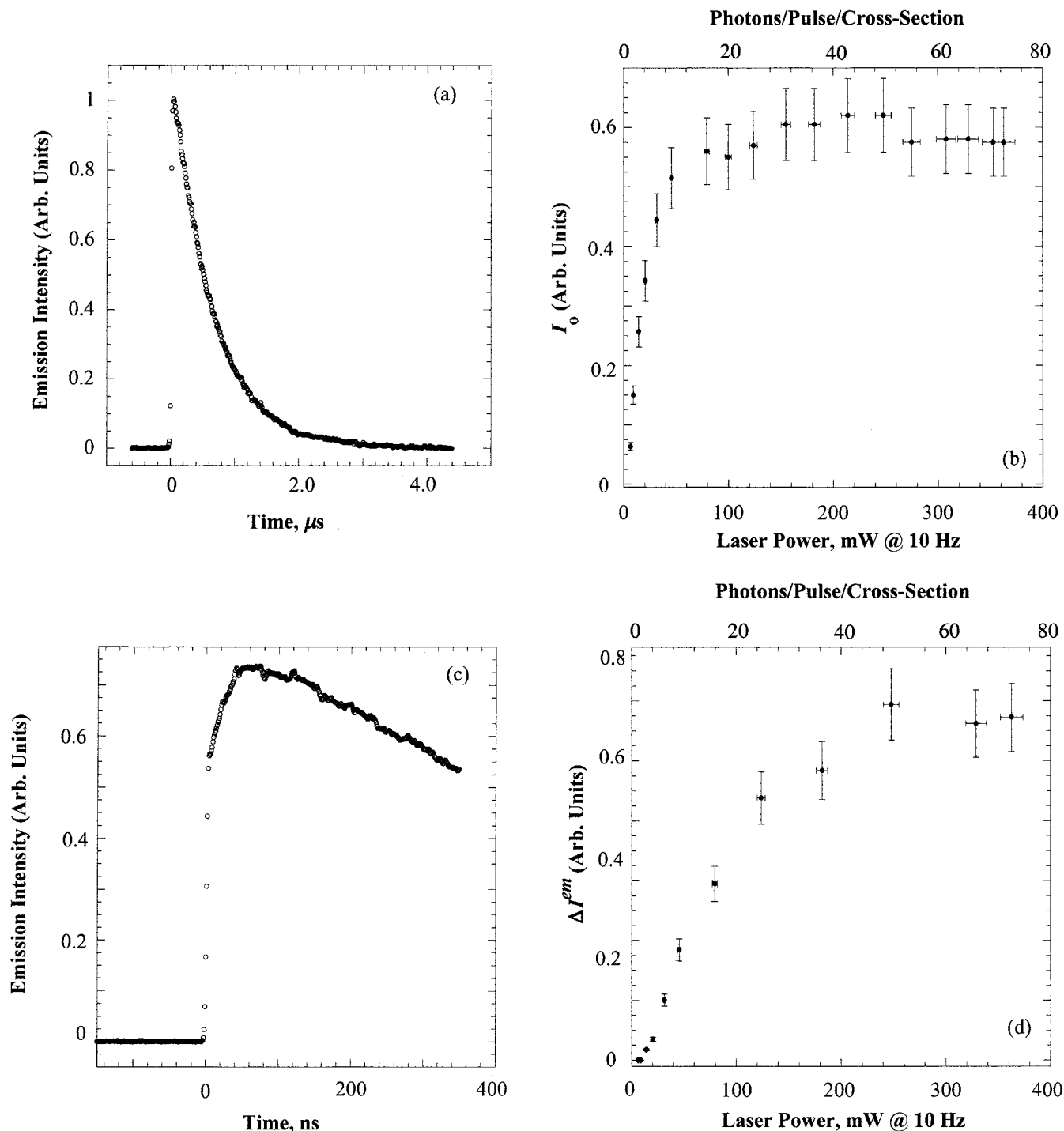


Figure 1. (a) Emission decay monitored at 620 nm following 355 nm pulsed laser excitation at 3.0 mJ/pulse for $[\text{Ru}^{\text{II}}(\text{bpy})_3]^{2+}$. (b) A plot of I_0^{Em} vs laser power for $[\text{Ru}^{\text{II}}(\text{bpy})_3]^{2+}$. Also plotted on the upper abscissa is the flux of photons per pulse per cross-sectional area of $[\text{Ru}^{\text{II}}(\text{bpy})_3]^{2+}$. The latter was estimated to be $5 \times 10^{-17} \text{ cm}^2/\text{molecule}$ from the molar absorptivity of $[\text{Ru}^{\text{II}}(\text{bpy})_3]^{2+}$. The laser beam diameter was $\sim 3 \text{ mm}$. (c) Time-resolved emission monitored at 620 nm for $[\text{Ru}^{\text{II}}(\text{bpy})_3]^{2+}$ following 6 ns pulsed laser excitation at 39.0 mJ/pulse. The time scale has been expanded to highlight the early time dynamics. (d) A plot of ΔI^{Em} (where $\Delta I^{\text{Em}} = I_{t=100\text{ns}}^{\text{Em}} - I_0^{\text{Em}}$ and $I_{t=100\text{ns}}^{\text{Em}}$ is the emission amplitude at 100 ns) as a function of laser power. Also plotted on the upper abscissa is the flux of photons per pulse per cross-sectional area of $[\text{Ru}^{\text{II}}(\text{bpy})_3]^{2+}$ as described in Figure 1b. All data plotted in Figure 1 were obtained with $5 \mu\text{M}$ $[\text{Ru}^{\text{II}}(\text{bpy})_3]\text{Cl}_2$ in Ar saturated H_2O at 298 K.

nm ($\epsilon_{460} = 2200 \text{ M}^{-1} \text{ cm}^{-1}$), respectively. The absorption of a second 355 nm photon produces a higher excited state, ${}^3[\text{Ru}^{\text{III}}(\text{bpy}^{\bullet-})(\text{bpy})_2]^{2+}$ (Scheme 1b), formed by promotion of the added electron in $\text{bpy}^{\bullet-}$. This state, which can be viewed as a higher lying ${}^3\text{MLCT}$ state, lies 5.6 eV above the ground state. The present studies reveal that the “zero” time ($\leq 5 \text{ ns}$) emission amplitude and the subsequent emission dynamics from ${}^3[\text{Ru}^{\text{III}}(\text{bpy}^{\bullet-})(\text{bpy})_2]^{2+}$ display a complex dependence on excitation power.

At laser powers $< 1 \text{ mJ/pulse}$, there is a low probability of photon capture by ${}^3[\text{Ru}^{\text{III}}(\text{bpy}^{\bullet-})(\text{bpy})_2]^{2+}$, and the time-resolved emission displays single exponential decay kinetics with a lifetime independent of excitation energy. This is shown in Figure 1a. The zero-time emission intensities determined from the first-order kinetic fits are directly proportional to the emission quantum yields and are plotted as a function of the excitation intensity as shown in Figure 1b. Similar power dependence was also found for the transient absorption spectra

monitored at 450 nm. The power dependence at low laser powers is consistent with absorption of a single photon to form the Franck–Condon $^1\text{MLCT}$ excited state followed by rapid intersystem crossing to form the $^3\text{MLCT}$ excited state as previously discussed.¹³ The capture of a second photon by $^3[\text{Ru}^{\text{III}}(\text{bpy}^{\bullet-})(\text{bpy})_2]^{2+}$ is negligible at low laser power, and consequently, the emission intensity displays a linear dependence on the laser power. When the laser power is increased, absorption of a second photon becomes important and the time dependence of the $[\text{Ru}(\text{bpy})_3]^{2+}$ emission becomes more complex as shown in Figure 1c. The emission decay shows an increase in intensity at early times ($0\text{--}5.0 \times 10^{-8}$ s). This rise becomes more prominent with increasing excitation energy, Figure 1(d). These kinetics were adequately fit to a biexponential expression with rate constants of $3.7 (\pm 0.4) \times 10^7 \text{ s}^{-1}$ and $1.9 (\pm 0.4) \times 10^6 \text{ s}^{-1}$. The slower process is assigned to the $^3\text{MLCT}$ decay. To the best of our knowledge, this is the first observation of rise-time kinetics for population of the $^3\text{MLCT}$ state following sequential two-photon absorption. The rise in emission intensity is interpreted as repopulation of the $^3\text{MLCT}$ based excited state from a higher lying excited state ($\tau = 2.7 \times 10^{-7}$ s), presumably a ^3dd state which is readily accessed following the absorption of a second photon by $^3[\text{Ru}^{\text{III}}(\text{bpy}^{\bullet-})(\text{bpy})_2]^{2+}$. The amplitude of the rise time kinetics display a sigmoidal dependence on laser power, Figure 1d, as is predicted for a sequential two photonic excitation mechanism.

Transient absorption difference spectra were determined in deoxygenated H_2O media under low and high laser intensities. Low power laser-flash photolysis experiments at 355 or 532 nm (<4 mJ/pulse) gave identical transient absorption spectra and kinetics that were assigned to decay of the $^3\text{MLCT}$ excited state. With increased laser energy the relaxation kinetics become biphasic at 350–500 nm, with the slower phase becoming more prominent with increasing energy. Transient absorption spectra obtained under saturation conditions where almost all of the $[\text{Ru}(\text{bpy})_3]^{2+}$ absorbs two 355 nm photons (50 mJ/pulse) are shown in Figure 2. Immediately following excitation, positive absorption features at 350 and 500 nm and a broad bleach centered at 450 nm were observed. The decay kinetics at 350, 450, and 500 nm were biphasic and are adequately fit to a biexponential decay with rate constants of $1.9 (\pm 0.4) \times 10^6 \text{ s}^{-1}$ and $1.3 (\pm 0.4) \times 10^4 \text{ s}^{-1}$. The rate constant for the initial fast phase is assigned to decay of the $^3\text{MLCT}$ excited state based on the kinetics and transient spectra. The second phase is significantly slower than either of the processes observed for the emission of the $^3\text{MLCT}$ at high laser powers. The transient absorbance changes do not have sufficient signal-to-noise to fit to three exponential decays. The intermediate implicated by the second phase is relatively long-lived with $\tau = 80 \mu\text{s}$; however, the transient signals do not fully recover to preexcitation levels. At 460 and 500 nm, the recovery was 90–95% of the total transient signal.

The Nature of the Short-Lived Intermediate. The short-lived intermediate (2.7×10^{-7} s) implied by the repopulation of the $^3\text{MLCT}$ state on the 100 ns time scale is assigned to a ^3dd excited state. A ^3dd state has been implicated by the temperature dependence of the nonradiative deactivation rate of the $^3\text{MLCT}$ state. The $^3\text{MLCT}$ state is believed to be able to form the ^3dd state by thermal activation. Because an antibonding e_g orbital is populated in the ^3dd state, it is expected to undergo rapid ligand loss as discussed in the Introduction. The kinetics of deactivation of the $^3\text{MLCT}$ excited-state cannot distinguish between formation of the ^3dd state being rate determining and a fast preequilibrium between the $^3\text{MLCT}$ and ligand field states

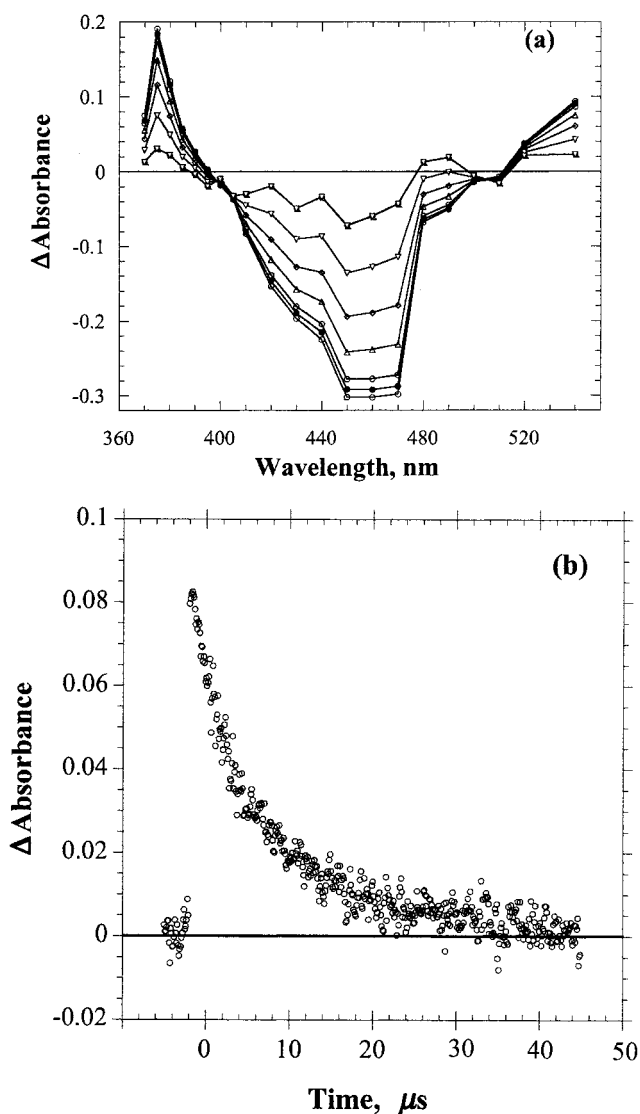
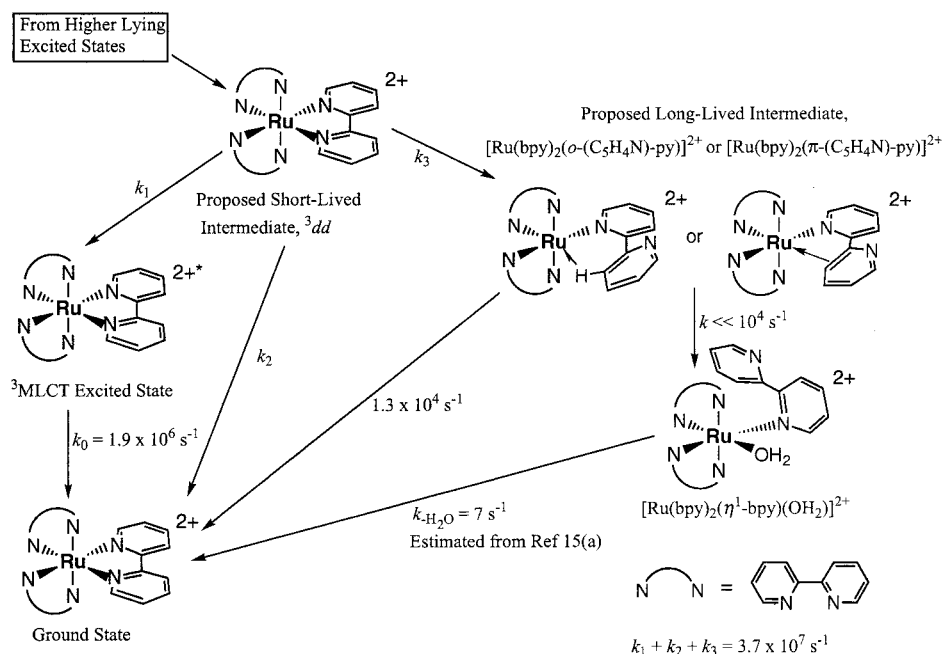


Figure 2. (a) Time-resolved transient absorption difference spectra for the intermediate formed following sequential two-photon absorption at 355 nm following 6 ns pulsed laser excitation at 39 mJ/pulse (3 mm laser beam diameter) on $5 \mu\text{M}$ $[\text{Ru}^{\text{II}}(\text{bpy})_3]\text{Cl}_2$ in Ar saturated H_2O at 298 K. The delay times for the recovery of the bleach at 460 nm are 0 ns, 200 ns, 7 μs , 19 μs , 36 μs , 66 μs , and 125 μs . (b) Time-resolved transient absorption trace for $[\text{Ru}^{\text{II}}(\text{bpy})_3]^{2+}$ monitored at 540 nm. All conditions are as described in Figure 2a.

followed by a slower deactivation of the ^3dd state. A detailed analysis of the kinetics will be presented elsewhere.^{12c} The ^3dd state is also assumed to be the precursor of the long-lived intermediate. Not all of the doubly excited state, $^3[\text{Ru}^{\text{III}}(\text{bpy}^{\bullet-})(\text{bpy})_2]^{2+}$, decays through the ^3dd state; rather, a significant portion of the doubly excited state directly repopulates the $^3\text{MLCT}$ state. This is suggested by our observation that the emission from the $^3\text{MLCT}$ state does not decrease significantly at the highest laser powers.

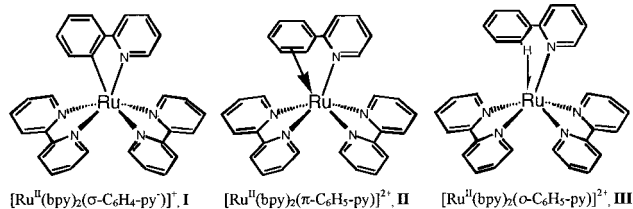
The Nature of the Long-Lived Intermediate. Evidence has been presented for the formation of a relatively long-lived intermediate (80 μs) by both laser flash photolysis and pulse radiolysis methods. It is reasonable that this intermediate is populated through the decay of the ^3dd excited state. The intermediate, which likely contains a monodentate bpy ligand, can either reform the ground state or lose the monodentate bpy. Our results suggest that the former pathway predominates at neutral pH.

SCHEME 2



Identification of the intermediate as an aquo complex $[\text{Ru}^{\text{II}}(\text{bpy})_2(\eta^1\text{-bpy})(\text{OH}_2)]^{2+}$ (where $\eta^1\text{-bpy}$ denotes a monodentate bpy) is ruled out by the following lines of evidence.¹⁵ The pentacoordinate $[\text{Ru}^{\text{II}}(\text{bpy})_2(\eta^1\text{-bpy})]^{2+}$ formed from the ^3dd state might rapidly add a H_2O molecule. It is known from extensive steady-state photolysis of $[\text{Ru}^{\text{II}}(\text{bpy})_3]^{2+}$ and $[\text{Ru}^{\text{II}}(\text{bpy})_2(\text{py})_2]^{2+}$ that nonradiative decay through the ^3dd state/s yield $[\text{Ru}^{\text{II}}(\text{bpy})_2(\eta^1\text{-bpy})(\text{X})]^{n+}$ and $[\text{Ru}^{\text{II}}(\text{bpy})_2\text{X}_2]^{n+}$ (where X = halide ($n = 1$) or coordinated solvent ($n = 2$)).¹⁵ Calculation of the transient spectra utilizing the known spectra for $[\text{Ru}^{\text{II}}(\text{bpy})_2(\text{py})(\text{OH}_2)]^{2+}$ or $[\text{Ru}^{\text{II}}(\text{bpy})_2(\text{OH}_2)_2]^{2+}$ are not consistent with the spectral data obtained in this work. Furthermore, the first-order kinetics observed in the flash photolysis experiments (see above) implicate a rate constant of $k \approx 10^4 \text{ s}^{-1}$ that is some 4–8 orders of magnitude faster than OH_2 dissociation from other Ru(II) polypyridyl complexes.¹⁵ It is therefore unlikely that the long-lived intermediate is a $[\text{Ru}^{\text{II}}(\text{bpy})_2(\eta^1\text{-bpy})(\text{X})]^{n+}$ -type species.

We propose that photocleavage of a Ru–N bond in $[\text{Ru}^{\text{II}}(\text{bpy})_3]^{2+}$ yields a $[\text{Ru}^{\text{II}}(\text{bpy})_2(\eta^1\text{-bpy})]^{2+}$ and that this is followed by rapid pyridyl ring rotation and/or transient formation of a long-lived $[\text{Ru}^{\text{II}}(\text{bpy})_2(\pi\text{-bpy})]^{2+}$ complex in which the pendant pyridyl ring is ligated in an η^2 or π fashion¹⁶ or through a weak C–H agostic interaction.¹⁷ Synthetic experiments where $\text{Ru}(\text{bpy})_2\text{Cl}_2$ was reacted with 2-phenylpyridine ($\text{C}_6\text{H}_5\text{-py}$) were undertaken to identify a coordination mode that could give rise to the observed transient spectroscopy. Three possible bonding modes for $[\text{Ru}^{\text{II}}(\text{bpy})_2(\text{C}_6\text{H}_5\text{-py})]^{2+}$ are shown below.



The $[\text{Ru}^{\text{II}}(\text{bpy})_2(\sigma\text{-C}_6\text{H}_4\text{-py}^-)]^+$ complex **I** has been prepared previously, and the crystal structure is known.^{18a} Complex **II**, the $[\text{Ru}^{\text{II}}(\text{bpy})_2(\pi\text{-C}_6\text{H}_5\text{-py})]^{2+}$ ion, has the phenyl moiety in $\text{C}_6\text{H}_5\text{-py}$ π -bonded in an η^2 fashion. A similar type of π -bonded

complex has been postulated as an intermediate in $[\text{Ru}(\text{NH}_3)_5(\text{py})]^{2+}$ flash photolysis studies by Ford,^{16a} and as an intermediate in the reduction of $[\text{Ru}(\text{NH}_3)_5(\text{isonicotinamide})]^{2+}$ complexes.^{16b,c} Numerous examples of η^2 -arene complexes of Os are known.^{16e} Chaudret has recently reported the synthesis and NMR and X-ray crystallographic characterization of $[\text{RuH}(\text{H}_2)(o\text{-C}_6\text{H}_5\text{-py})(\text{P}^i\text{R}_3)_2]^+$, a structural analogue of **III**, which clearly show the agostic C–H bonding interaction involving the $\text{C}_6\text{H}_5\text{-py}$ moiety.¹⁷

A red material tentatively assigned as the $[\text{Ru}^{\text{II}}(\text{bpy})_2(o\text{-C}_6\text{H}_5\text{-py})]^{2+}$, **III**, complex has been isolated and characterized by NMR in this work.¹⁹ The visible absorption spectrum is distinctly different than that reported for $[\text{Ru}^{\text{II}}(\text{bpy})_2(\sigma\text{-C}_6\text{H}_4\text{-py}^-)]^+$ and is atypical of $[\text{Ru}^{\text{II}}(\text{bpy})_2(\text{py})\text{L}]^{2+}$ ($\text{L} = \text{py}$ and OH_2) complexes. The low-energy band is extremely broad ($\Delta\nu_{1/2} = 5250 \text{ cm}^{-1}$) and featureless with little evidence for the vibronic progressions which appear as shoulders on the high energy side of the MLCT envelope as seen in $[\text{Ru}^{\text{II}}(\text{bpy})_3]^{2+}$ and $[\text{Ru}^{\text{II}}(\text{bpy})_2(\text{py})\text{L}]^{2+}$ derivatives. The ^1H NMR spectrum of $[\text{Ru}^{\text{II}}(\text{bpy})_2(o\text{-C}_6\text{H}_5\text{-py})]^{2+}$ in CD_3OD is complex, as expected for 25 magnetically inequivalent protons. The resonance tentatively assigned to the agostic C–H is a broad singlet at 6.6 ppm (8.1 ppm for free $\text{C}_6\text{H}_5\text{-py}$) in the ^1H NMR, a singlet at 117 ppm in the ^{13}C $\{^1\text{H}\}$ decoupled NMR spectrum, and appears as a doublet in the ^{13}C NMR with $J_{\text{C-H}} = 158 \text{ Hz}$. The value of $J_{\text{C-H}}$ for the putative agostic proton at room temperature is only slightly shifted from $J_{\text{C-H}} = 165 \text{ Hz}$ for the aryl C–H in $[\text{Ru}^{\text{II}}(\text{bpy})_2(o\text{-C}_6\text{H}_5\text{-py})]^{2+}$ and is significantly larger than $J_{\text{C-H}} = 128 \text{ Hz}$ in $[\text{RuH}(\text{H}_2)(o\text{-C}_6\text{H}_5\text{-py})(\text{P}^i\text{R}_3)_2]^+$ at 173 K.^{17b} The magnitude of $J_{\text{C-H}}$ in **III** suggests that if there is an agostic interaction it is weak.¹⁷ Full preparative details and characterization data for $[\text{Ru}(\text{bpy})_2(o\text{-C}_6\text{H}_5\text{-py})](\text{PF}_6)$ will be published elsewhere.^{12c}

Photochemical Mechanism. The model for excited-state decay of $[\text{Ru}^{\text{II}}(\text{bpy})_3]^{2+}$ that emerges from the results reported here is summarized in Scheme 2. The emissive $^3\text{MLCT}$ excited states can be populated via (a) monophotonic MLCT excitation and rapid intersystem crossing (the “standard” model), (b) relaxation from the electron adduct $[\text{Ru}(\text{bpy})_3]^{3+}/e_{\text{aq}}^-$, or (c) sequential two-photon absorption with high power 355 nm

excitation. Accordingly, enhanced population of the ^3dd excited state has been achieved both via relaxation from the electron adduct $[\text{Ru}(\text{bpy})_3]^{3+}/e_{\text{aq}}^-$ and by a sequential two-photon absorption mechanism. The ^3dd excited state can decay by (i) back intersystem crossing to the $^3\text{MLCT}$ as evidenced by the emission rise time kinetics observed at high laser powers, (ii) direct deactivation to the ground state, and (iii) Ru–pyridyl bond cleavage and ligand rearrangement to form a transient π -bonded or agostic species which then undergoes ligand rearrangement to reform $[\text{Ru}(\text{bpy})_3]^{2+}$ with a lifetime of 80 μs . This is a significant result because it suggests that photochemical catalysts that activate C–H bonds might be achieved in appropriately designed Ru(II) polypyridyl complexes.²⁰

Finally, these observations call into question some of the previous assumptions regarding ^3dd excited-state decay in $[\text{Ru}(\text{bpy})_3]^{2+}$. The ^3dd excited states of $[\text{Ru}(\text{bpy})_3]^{2+}$ have lifetimes in the nanosecond regime and are much longer lived than previously thought. Although the ^3dd states are highly reactive toward ligand loss in aqueous media, the dominant decay route is reformation of $[\text{Ru}(\text{bpy})_3]^{2+}$ and only a relatively small amount of the complex is trapped as aquo species; thus, there is very little net photochemistry under normal conditions. The quantum yields for photosubstitution in aqueous media are a poor indication of the extent of excited-state decay that proceeds through metal-centered excited states.

Acknowledgment. The authors thank Edward. W. Castner, Jr., Morris Bullock, Carol Creutz, and Prasenjit Ghosh for valuable discussions. This research was carried out at Brookhaven National Laboratory under Contract DE-AC02-98-CH1088 with the U.S. Department of Energy and is supported by its Division of Chemical Sciences, Office of Basic Energy Sciences.

References and Notes

- (1) Roundhill, D. M. *Photochemistry and Photophysics of Metal Complexes*. In *Modern Inorganic Chemistry*; Fackler, J. P., Ed.; Plenum Press: New York, 1994. (b) Kalyanasundaram, K. *Photochemistry of Polypyridine and Porphyrin Complexes*; Academic: New York, 1992. (c) Balzani, V.; Juris, A.; Venturi, M.; Campagna, S.; Serroni, S. *Chem. Rev.* **1996**, *96*, 759–833. (d) Juris, A.; Balzani, V.; Barigelletti, F.; Campagna, S.; Belser, P.; Von Zelewsky, A. *Coord. Chem. Rev.* **1988**, *84*, 85–277. (e) Meyer, T. J. *Pure Appl. Chem.* **1986**, *58*, 1193–1206. (f) Chen, P. Y.; Meyer, T. J. *Chem. Rev.* **1996**, *96*, 759–833.
- (2) (a) Yeh, A. T.; Shank, C. V.; McCusker, J. K. *Science* **2000**, *289*, 935. (b) Damrauer, N. H.; Cerulo, G.; Yeh, A. T.; Boussie, T. R.; Shank, C. V.; McCusker, J. K. *Science* **1997**, *275*, 54.
- (3) Bigozzi, C. A.; Schoonover, J. R.; Scandola, F. A. *Prog. Inorg. Chem.* **1997**, *44*, 1–96 and references therein.
- (4) (a) Islam, A.; Ikeda, N.; Yoshimura, A.; Ohno, T. *Inorg. Chem.* **1998**, *37*, 3093–3098. (b) Barqawi, K. R.; Llobet, A.; Meyer, T. J. *J. Am. Chem. Soc.* **1988**, *110*, 7751–7759 and references therein.
- (5) (a) Lakowicz, J. R.; Castellano, F. N.; Gryczynski, I.; Gryczynski, Z.; Dattelbaum, J. D. *J. Photochem. Photobiol. A* **1999**, *122*, 95–101. (b) Castellano, F. N.; Malak, H.; Gryczynski, I.; Lakowicz, J. R. *Inorg. Chem.* **1997**, *36*, 5548–5551. (c) Berger, R. M.; McMillin, D. R.; Dallinger, R. F. *Inorg. Chem.* **1987**, *26*, 3802–3805. (d) Meisel, D.; Matheson, M. S.; Rabani, J. *J. Am. Chem. Soc.* **1978**, *100*, 117–122. (e) Meisel, D.; Matheson, M. S.; Mulac, W. A.; Rabani, J. *J. Phys. Chem.* **1977**, *81*, 1449. (f) Ballardini, R.; Gandolfi, M. T.; Balzani, V. *J. Phys. Chem.* **1988**, *92*, 56–60. (g) Nocera, D. G. *Acc. Chem. Res.* **1995**, *28*, 209–217.
- (6) Jonah, C. D.; Matheson, M. S.; Meisel, D. *J. Am. Chem. Soc.* **1978**, *100*, 1449.
- (7) (a) Naik, D. B.; Schnabel, W. *Chem. Phys. Lett.* **1999**, *315*, 416–420. (b) Naik, D. B.; Schnabel, W. *Chem. Phys. Lett.* **1994**, *228*, 1110. (c) Atherton, S. J. *J. Phys. Chem.* **1984**, *88*, 2840–2844.
- (8) (a) Creutz, C.; Sutin, N. *J. Am. Chem. Soc.* **1976**, *98*, 6384. (b) Ferraudi, G.; Arguello, G. A. *Inorg. Chem. Acta* **1998**, *144*, 53–55. (c) Milosavijevic, B. H.; Thomas, J. K. *J. Phys. Chem.* **1983**, *87*, 616–621.
- (9) Winkler, J. R.; Netzel, T. L.; Creutz, C.; Sutin, N. *J. Am. Chem. Soc.* **1987**, *109*, 2381–2392.
- (10) Electron pulse-radiolysis transient-absorption experiments were carried out at the 2 MeV Van de Graaff accelerator (50–200 ns electron pulses) at Brookhaven National Laboratory. The irradiations were carried out at 22 (± 2) °C on samples contained in 2 cm path length Supracil cells

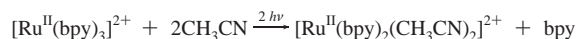
(cell dimensions were $2 \times 1 \times 0.5$ cm). The probe beam was generated by a 75 W Xe arc lamp which was pulsed for measurement times less than 10^{-4} s. Faster time-resolved electron pulse-radiolysis experiments were carried out at the 9 MeV Laser Electron Accelerator Facility (LEAF) at Brookhaven National Laboratory. The experimental details regarding LEAF will be presented elsewhere.

(11) (a) The pulse radiolysis experiments were hampered by the instability of $[\text{Ru}(\text{bpy})_3]^{3+}$ towards thermal and photochemical decomposition.^{11b} A prepulse flow system was used to keep the $[\text{Ru}^{\text{III}}(\text{bpy})_3]^{3+}$ reactant solution at low pH. Immediately before the pulse, the acidic ruthenium solution was mixed with acetate buffer. (b) Ghosh, P. K.; Brunschwig, B. S.; Chou, M.; Creutz, C.; Sutin, N. *J. Am. Chem. Soc.* **1984**, *106*, 4772–4783.

(12) Transient absorption spectra and lifetimes were measured using a modified apparatus described elsewhere.^{12b,c} Excitation was provided by primarily the third harmonic ($\lambda_{\text{exc}} = 355$ nm, 6 ns pulse-width, 0–50 mJ/pulse) from a Continuum Surelite-1 Nd:Yag laser. The laser spot size was ~ 3 mm in diameter at the sample. All experiments were performed at 25 °C. (b) Hamada, T.; Brunschwig, B. S.; Eifuku, K.; Fujita, E.; Korner, M.; Sakaki, S.; van Eldik, R.; Wishart, J. F. *J. Phys. Chem. A* **1999**, *103*, 5645–5654. (c) Thompson, D. W.; Wishart, J. F.; Brunschwig, B. S.; Sutin, N. Manuscript in preparation.

(13) (a) Lachish, U.; Shafferman, A.; Stein, G. *J. Chem. Phys.* **1976**, *64*, 4205–4211. (b) Yoshimura, A.; Hoffman, M. Z.; Sun, H. *Photochem. Photobiol. A: Chem.* **1993**, *70*, 29–33. (c) Creutz, C.; Chou, M.; Netzel, T. L.; Okumura, M.; Sutin, N. *J. Am. Chem. Soc.* **1980**, *102*, 1309–1319. (d) Van Vlietberge, B.; Ferraudi, G. *Inorg. Chem.* **1987**, *26*, 337–340.

(14) With monophotonic excitation at 460 nm, Whitten et al. demonstrated that photochemical displacement of bpy by CH_3CN was inefficient with $\phi_{\text{bpy}} < 10^{-4}$.^{14b} Consistent with this, we find negligible changes in the absorption spectra after steady-state excitation of $[\text{Ru}^{\text{II}}(\text{bpy})_3]^{2+}$ in CH_3CN solution with 4×10^4 low-power ($3\text{--}5$ mJ pulse $^{-1}$) 355 nm laser pulses. When the laser pulse energy was increased to 50 mJ pulse $^{-1}$, facile spectral changes were observed with bleaching of the MLCT absorption at 452 nm and appearance of a new band at 426 nm. These changes are consistent with the sequential absorption of two photons:



The $[\text{Ru}^{\text{II}}(\text{bpy})_2(\text{CH}_3\text{CN})_2]^{2+}$ presumably arises via bpy loss from the ^3dd state which is efficiently populated following on two-photon absorption. No evidence for photoejection of an electron was found under the conditions used in the present work. (b) Foreman, T. K.; Bonilha, J. P. B.; Whitten, D. G. *J. Phys. Chem.* **1982**, *86*, 3436.

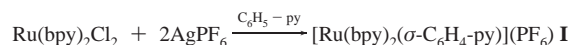
(15) (a) Tachiyashiki, S.; Nakamaru, K.; Mizumachi, K. *Chem. Lett.* **1992**, 1119–1122. (b) Tachiyashiki, S.; Ikezawa, H.; Mizumachi, K. *Inorg. Chem.* **1994**, *33*, 623–625. (c) Arakawa, R.; Tachiyashiki, S.; Matsuo, T. *Anal. Chem.* **1995**, *67*, 4133–4138. (d) Luo, J.; Bal Reddy, K.; Salameh, A. S.; Wishart, J. W.; Isied, S. S. *Inorg. Chem.* **2000**, *39*, 2321–2329. (e) Allen, L. R.; Craft, P. P.; Durham, B.; Walsh, J. *Inorg. Chem.* **1987**, *26*, 53–56.

(16) (a) Durante, V. A.; Ford, P. C. *Inorg. Chem.* **1979**, *18*, 588–593. (b) Chou, M. H.; Brunschwig, B. S.; Creutz, C.; Sutin, N.; Yeh, A.; Chang, R. C.; Lin, C.-T. *Inorg. Chem.* **1992**, *31*, 5347–5348. (c) Chou, M. H.; Szalda, D. J.; Creutz, C.; Sutin, N. *Inorg. Chem.* **1994**, *33*, 1674–1684. (d) Sullivan, B. P.; Bauman, J. A.; Meyer, T. J.; Salmon, D. J.; Lehmann, H.; Ludi, A. *J. Am. Chem. Soc.* **1977**, *99*, 7368–7369. (e) Harman, W. D. *Chem. Rev.* **1997**, *97*, 1953–1978.

(17) (a) Brookhart, M.; Green, M. H.; Wong, L. *Prog. Inorg. Chem.* **1988**, *36*, 1–115. (b) Toner, A. J.; Grundemann, S.; Clot, E.; Limbach, H.; Donnadiue, B.; Sabo-Etienne, S.; Chaudret, B. *J. Am. Chem. Soc.* **2000**, *122*, 6777–6778.

(18) (a) Constable, E. C.; Holmes, J. M. *J. Organomet. Chem.* **1986**, *301*, 203–208. (b) Reveco, P.; Medley, J. H.; Garber, A. R.; Bhacca, N. S.; Selbin, J. *Inorg. Chem.* **1985**, *24*, 1096–1099. (c) Reveco, P.; Schmeil, R. H.; Cherry, W. R.; Fronczek, F. R.; Selbin, J. *Inorg. Chem.* **1986**, *25*, 1842–1845. (d) Reveco, P.; Cherry, W. R.; Medley, J. H.; Garber, A. R.; Gale R. J.; Selbin, J. *Inorg. Chem.* **1986**, *25*, 1842–1845.

(19) Briefly, when following the protocols outlined by Constable and Holmes



for the synthesis of $[\text{Ru}(\text{bpy})_2(\sigma\text{-C}_6\text{H}_4\text{-py})](\text{PF}_6) \text{ I}$,^{18a} two compounds were isolated from recrystallization in MeOH. The first compound (>70% yield) was a black crystalline material which was MeOH insoluble and was identified as $[\text{Ru}(\text{bpy})_2(\sigma\text{-C}_6\text{H}_4\text{-py})](\text{PF}_6) \text{ I}$, based on the previously published visible and ^1H NMR spectra in DMSO- d_6 solution. The second compound was a red material (<12% yield) that was tentatively assigned as $[\text{Ru}(\text{bpy})_2(\sigma\text{-C}_6\text{H}_5\text{-py})](\text{PF}_6) \text{ III}$, based on a detailed analysis of the ^1H NMR, ^{13}C NMR, and $^{13}\text{C}\{^1\text{H}\}$ NMR spectra obtained in CD_3OD using a 400 MHz Bruker spectrometer.

(20) Asbury, J. B.; Hang, K.; Yeston, J. S.; Cordaro, J. G.; Bergman, R. G.; Lian, T. *J. Am. Chem. Soc.* **2000**, *122*, 12870–12871 and references therein.